

A general phase-field framework for (de)wetting

A. Voigt (Technische Universität Dresden)

0 Summary

Dewetting phenomena are universal and have been observed on a variety of inorganic and organic materials (such as liquids, polymers, metals and semiconductors). While liquid films are in the focus of the SPP 2171, dewetting is also relevant for solid thin films, where some of the underlying physical processes are very similar. We therefore consider a general phase field modeling approach for dewetting of liquid/viscoelastic/elastic thin films on liquid/viscoelastic/elastic substrates, which allows to identify similarities and differences. The model is based on research on multiphase flow with moving contact lines, including surfactants, surface viscosity, non-Newtonian fluids and complex topographies as well as models for surface diffusion, bulk and surface elasticity and viscoelastic materials, which will be combined in a general multiphase field model. These models are implemented in AMDiS, a user-friendly adaptive finite element toolbox for high performance computing, demonstrated to scale up to several thousand processors, which will also be used for this project and provided to other groups of the SPP2171. We extend these modeling approaches, which consider the extreme cases of Young and Neumann condition at the contact line to more general situations by including surface stresses and analyze the influence of elastocapillarity. We develop surface elastic and viscoelastic models and improve numerical approaches to solve them. With these extensions the framework can be applied to specific applications with flexible, adaptive and switchable substrates. The models will be validated with other theoretical and experimental projects within the SPP2171. We further plan to develop various benchmark problems.

1 State of the art and preliminary work

1.1 General

Thin films on (soft) substrates are ubiquitous in nature and technology. We find them on plant leaves when it rains, they line our lungs and form the tear film that protects our eyes, but they are also essential for coating and printing techniques and various nanotechnology applications. Here we will focus on dewetting of thin films, which is a spontaneous phenomenon where the thin film on a substrate rearranges itself into an ensemble of separated objects.

In several instances, dewetting phenomena are undesirable as in the rupture of a protective coating or paint or within metal silicides or silicon-on-insulator structures in integrated circuits. However, there is an increasing number of examples in which dewetting has been purposely induced, e.g. on omniphobic surfaces, to pattern nanoparticles in functional devices, to make particle arrays in sensors, to form elements in electrical memory devices or to self-assemble nanowires. For all these applications controlling dewetting would be highly desirable.

Dewetting phenomena are universal and have been observed on a variety of inorganic and organic materials (such as liquids, polymers, metals and semiconductors). While liquid films are in the focus of the SPP 2171, dewetting is also relevant well below the film's melting temperature, a phenomenon known as solid state dewetting. Driven by the technological importance of the dewetting phenomena, both for liquid and solid thin films, a significant modeling and experimental literature on this topic exists. We refer to [19, 55, 61] for general reviews, which also contain most of the mentioned examples above. The research on liquid and solid thin films is

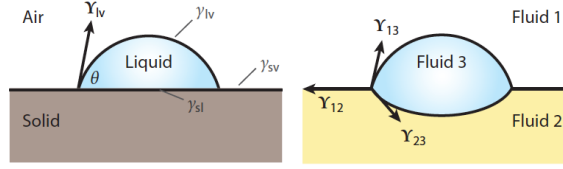


Figure 1: Relation between surface energies γ_{ij} , surface stresses Υ_{ij} and contact angles θ_i . (left) Young's equation - two deformable phases on rigid substrate, (right) Neumann's triangle relation - three deformable phases. Image from [55].

until today mainly distinct from each other, even if some of the underlying physical processes are very similar. While our main focus will be on liquid thin films, we will relate this research also to solid thin films with the goal to identify common phenomena, similarities and differences.

1.2 Modeling and simulation

The dynamics of drops and liquid thin films is often described by approximate models, the so called thin-film equations. Considering the viscosity and the disparity between horizontal and vertical length scales allows to derive these equations by a lubrication approximation of the basic transport equations of physico-chemical hydrodynamics. Excellent agreement of the spatial and temporal evolution of the rupture of ultrathin polystyrene films could e.g. be achieved with these models [9]. More recent results consider more complex fluids and reformulate these models as gradient flows. Similar long-wave length expansions can also be considered for thin solid films. However, the limitations of these approaches become essential if applied to more complex materials relevant in modern applications, where the dewetting process might lead to morphologies unable to be described by a height function. We will therefor not rely on thin-film equations but consider the full transport equations and only use the approximation to relate our results to our groups in the SPP2171.

Most work until today has been done for rigid substrates, where the equilibrium configuration of a droplet is determined by local energy balance represented by Young's equation. This holds for liquid as well as solid droplets, at least if only isotropic surface energies are considered. Minimizing the interfacial energy of the droplet/substrate system, one finds that the contact angle θ depends only on the surface energies of the three interfaces γ_{lv} , γ_{sv} and γ_{sl} through

$$\cos \theta = \frac{\gamma_{lv} - \gamma_{sl}}{\gamma_{sv}}, \quad (1)$$

see Figure 1(left). If all three phases are deformable the sum of all forces acting on the triple line is zero in equilibrium and the force vectors form a triangle. The relation between the magnitude of the forces and their angles reads

$$\frac{\gamma_{13}}{\sin \theta_2} = \frac{\gamma_{12}}{\sin \theta_3} = \frac{\gamma_{23}}{\sin \theta_1}, \quad (2)$$

which is known as Neumann's triangle relation, see Figure 1(right). Eqs. (1) and (2) have served as a basis for understanding the static structure and dynamics of droplets over many years, see e.g. [13]. Various modeling approaches which rely on these conditions exist. We will here only review the state of the art in phase field modeling related to eqs. (1) and (2). On rigid substrates an appropriate description is given by a Cahn-Hilliard equation with an order parameter ϕ distinguishing between liquid and air and an additional order parameter ψ given by $\psi(z) = \frac{1}{2}(1 - \tanh(\frac{3z}{\epsilon}))$, with z the height above the substrate and ϵ an interface width. The equation results as a conserved gradient flow of the free energy $\mathcal{F} = \mathcal{F}_{GL} + \mathcal{F}_{substrate}$ with a

Ginzburg-Landau and a substrate term, with

$$\mathcal{F}_{GL}[\phi] = \int_{\Omega} \gamma_{lv} \left(\frac{\epsilon}{2} |\nabla \phi|^2 + \frac{1}{\epsilon} B(\phi) \right) d\Omega \quad (3)$$

$$\mathcal{F}_{substrate}[\phi] = \int_{\Omega} \frac{1}{\epsilon} B(\psi) \left(\frac{1}{2} (\gamma_{sv} + \gamma_{sl}) - \frac{-4\phi^3 + 6\phi^2 - 1}{2} (\gamma_{sv} - \gamma_{sl}) \right) d\Omega \quad (4)$$

and reads

$$\partial_t \phi = \nabla \cdot \left(\frac{1}{\epsilon} M(\phi) \nabla \mu \right), \quad \mu = \gamma_{lv} (-\epsilon \Delta \phi + \frac{1}{\epsilon} B'(\phi)) + \frac{1}{\epsilon} B(\psi) 6\phi(\phi - 1)(\gamma_{sv} - \gamma_{sl}) \quad (5)$$

with chemical potential $\mu = \frac{\delta \mathcal{F}}{\delta \phi}$, quartic double-well potential $B(\phi) = 18\phi^2(1 - \phi)^2$ and mobility function $M(\phi)$, which can be used to distinguish between various mass transport mechanisms, e.g. bulk diffusion ($M(\phi) = \epsilon$ for liquid droplets), surface diffusion ($M(\phi) = 36\phi^2(1 - \phi)^2$ for solid droplets) or intermediate regimes, see e.g. [1, 12, 63]. For $\epsilon \rightarrow 0$ the model converges to the desired evolution equations with Young's equation as boundary condition [15] and [P1]. The approach can easily be adapted to different topographies by changing the definition of ψ . More detailed descriptions taking the specific physico-chemical processes for liquids and solids into account, couple this model with hydrodynamics or elasticity in the bulk phases. A general concept how to derive phase field models with coupled bulk and surface phenomena is derived in [28, 41, 58]. For liquid droplets that leads to a Cahn-Hilliard-Navier-Stokes equation, whereas for solid droplets a Cahn-Larche type system results. A huge mathematical literature exists on modeling issues, asymptotic analysis and numerical analysis for these equations. However, already for this relatively simple situation the understanding is not complete. For two-phase flows there are still ongoing controversially discussions on advantages and disadvantages of mass- or volume-averaged approaches for situations of high density ratios between the phases, see e.g. [2, 29, 44]. Besides these modeling aspects the development of appropriate solvers is a current research focus in numerical mathematics. For all of the available models large scale three-dimensional simulations are still rare.

Also Neumann's triangle relation can be considered within a phase field model. Here it is appropriate to use a multi-phase field approach with phases ϕ_1, ϕ_2, \dots being 1 in phase 1, 2, ..., respectively and 0 otherwise and an algebraic constraint $\sum_{i=1}^N \phi_i = 1$, with $N = 3$ in the case considered above, see e.g. [54] for a review. The free energy for $\phi = (\phi_1, \phi_2, \dots)$ now reads

$$\mathcal{F}[\phi] = \int_{\Omega} \frac{\epsilon}{2} \sum_{i,j=1}^N \Lambda_{ij} \nabla \phi_i \cdot \nabla \phi_j + \frac{1}{\epsilon} f(\phi) d\Omega \quad (6)$$

with $f(\phi) = f_1(\phi) + s f_2(\phi)$,

$$f_1(\phi) = \sum_{i,j=1}^N \gamma_{ij} (\hat{f}(\phi_i) + \hat{f}(\phi_j) - \hat{f}(\phi_i + \phi_j)), \quad f_2(\phi) = \sum_{i,j=1}^N \gamma_{ij} \phi_i^2 \phi_j^2 \sum_{k \neq i,j} \phi_k^2 \quad (7)$$

and $\hat{f}(\phi) = \phi^2(1 - \phi)^2$, $\gamma_{ii} = 0$, $\gamma_{ij} = \gamma_{ji}$, Λ a coupling matrix and s a scaling parameter. The evolution equation follows again as an appropriate gradient flow taking the specific mass transport mechanisms into account. Neumann's triangle relation follows naturally in equilibrium. Also these models can be coupled in the same way as described before with physico-chemical processes within the bulk phases, considering different liquid or solid properties in each phase, which leads to the same modeling and numerical issues as mentioned above.

While Young's equation and Neumann's triangle relation are well established contact angle conditions, it recently became apparent that wetting on soft substrates cannot be described by either of these cases. The two conditions can only be seen as limits of a more general relation to be discussed in the next section.

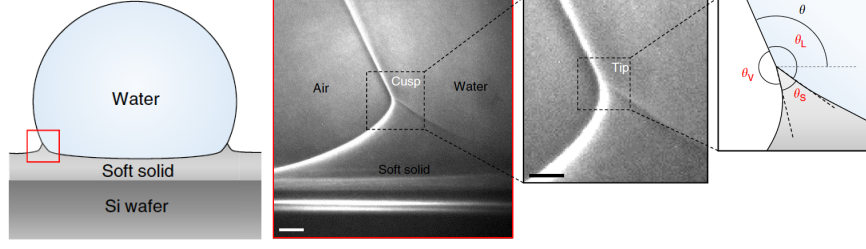


Figure 2: High-resolution X-ray imaging for ridge formation of a water droplet on a silicon gel, together with the microscopic contact angles θ_S , θ_V and θ_L and the macroscopic contact angle θ . The scale bars are 2 (white) and 1 (black) μm . Image from [38].

1.3 Scientific developments during the last years

The surface of a material has an energy penalty per unit area of surface, the surface energy γ . In liquids this gives rise to a tensile surface stress Υ , that opposes surface stretching. It acts to minimize the surface-to-volume ratio and is the source of the Laplace pressure difference across curved surfaces. Υ is a symmetric second-order, two-dimensional tensor. However, in simple liquids it is isotropic $\Upsilon = \Upsilon \mathbf{I}$ and it holds that $\gamma = \Upsilon$. For solids this is no longer true, as the surface energy becomes strain-dependent, the so-called Shuttleworth effect [50]. For a general continuum theory of elastic material surfaces we refer to [20]. Just as the surface energy creates a jump in the hydrostatic pressure across a curved interface in liquids, the surface stress causes a jump in the stress across a solid interface, which drives local deformations in the bulk of the solid. For an elastic solid with Young's modulus E we expect significant deformations when $\frac{1}{H} \sim \frac{\Upsilon}{E}$, with H the mean curvature and $\frac{\Upsilon}{E}$ the elastocapillary length. For scales much larger than $\frac{\Upsilon}{E}$ surface effects are negligible and at scales much smaller than $\frac{\Upsilon}{E}$ surfaces stresses dominate. On a continuum level such phenomena are possible only if $\frac{\Upsilon}{E}$ is much larger than molecular scales, which is e.g. the case for gels and elastomers. For these cases characteristic rim shapes are formed and the dynamics of the dewetting process is influenced [38, 48], see Figure 2.

The equilibrium condition to be satisfied at the interface between two deformable phases is

$$(\sigma_1 - \sigma_2) \cdot \mathbf{n} = -\nabla_\Gamma \cdot \Upsilon, \quad (\sigma_1 - \sigma_2) \cdot \mathbf{n} = \Upsilon H \mathbf{n} - \nabla_\Gamma \Upsilon, \quad (8)$$

for the general and the isotropic case, respectively. $\sigma_{1,2}$ are the Cauchy stresses in the deformed bulk phases and \mathbf{n} the surface normal. The first term in the isotropic setting is normal to the interface, while the second is in-plane and corresponds to Marangoni stresses in liquids. Most theoretical investigations consider only the first term. For this case a phase field approximation was recently developed using the tools from [28, 41, 58], see [32]. It considers a generalized Oldroyd-B model and allows to model liquid, elastic solid, viscoelastic Kelvin-Voigt and viscoelastic Maxwell phases. However, contact angle conditions have not been considered in this approach. An appropriate contact angle condition has to take into account that also Υ_{lv} deforms the soft solid substrate. It thus requires to consider a force balance between bulk and surface stresses in a small volume around the contact line

$$\int_{\Omega_1} \sigma_1 \cdot \mathbf{n}_1 d\Omega_1 + \int_{\Omega_2} \sigma_2 \cdot \mathbf{n}_2 d\Omega_2 + \int_{\Omega_3} \sigma_3 \cdot \mathbf{n}_3 d\Omega_3 + \Upsilon_{12} \cdot \mathbf{t}_{12} + \Upsilon_{13} \cdot \mathbf{t}_{13} + \Upsilon_{23} \cdot \mathbf{t}_{23} = 0, \quad (9)$$

see Figure 3. If the volume shrinks to zero and the bulk stresses are bounded this relation reduces to Neumann's triangle relation. Within a phase field approach a natural length scale, the diffuse interface width ϵ , determines the lower bound for the volume and will need to be chosen in the order of the molecular size to resolve the deformation at the contact line. A general mechanical theory combining bulk and surfaces stresses was proposed in [21]. For more recent approaches on nonlinear surface elasticity we refer e.g to [33, 64]. However, numerical

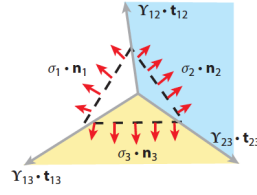


Figure 3: Force balance between bulk and surface stresses to be satisfied at contact line. The surface stress tensor and the tangent vector of the interface between phase i and j are Υ_{ij} and \mathbf{t}_{ij} , respectively, and the bulk stresses and normals σ_i and \mathbf{n}_i , respectively. Image from [55].

realization of these models in a general setting are rare, see e.g. [22] for first steps in this direction using tangential differential calculus. Similar approaches have recently been used for Kirchhoff-Love shell models [45] and can be extended to other shell theories. The numerical approach follows the same idea as considered in [35] for general tensor-valued surface partial differential equations and can be adapted to the surface setting.

Besides these equilibrium conditions also dynamics of contact lines have to be considered. In typical wetting and dewetting processes the contact angle becomes dynamic as well and can change considerably from its static value. Already in the simplest case of a liquid droplet on a rigid substrate fundamental mathematical problems arise as the setting with a no-slip condition for the velocity possesses no solution in the physically relevant class of smooth bounded solutions and dynamic contact angle conditions are still poorly understood. An overview of the available approaches is given in [49]. One of the few models, which considers the overall physical context of the moving contact line problem is Shikhmurzaev's interface formation model. In addition to keeping the problem well-posed, the contact angle is determined as part of the solution rather than being prescribed as a function of contact line speed, see [52] for a realization. We are not aware of a similar model for liquid droplets on soft substrates. Here the deformation of the substrate as a result of the droplet interaction creates a new source of dissipation, called viscoelastic braking. This can dominate the motion of the contact line, causing droplets to slide more slowly on a soft substrate than on a stiff substrate [48]. In modeling approaches the velocity of the advancing contact line is directly related to the substrate viscoelasticity [26, 27]. Other effects which drive contact line motions are gradients in the stiffness of soft substrates [56]. However, detailed modeling approaches of these phenomena do not exist.

Further model extensions consider more detailed description of the liquid/vapor interface. Surfactants, soluble or insoluble, can be of interest, as they lead to inhomogeneous surface energies and additional Marangoni fluxes in the bulk which influence the dynamics. For a phase field realization of two-phase flow with surfactants we refer to [59]. Also particle laden interfaces can lead to significant changes in the stress state and strongly influence the bulk flow. For a phase field realization modeling colloidal particles at interfaces see [5, 6]. Other approaches consider also the surface viscosity, with similar effects on the dynamics of the contact line. For modeling and numerical realizations of surface hydrodynamics see [37, 42, 43]. However, we are not aware of any systematic study of these effects in the context of (de)wetting.

In terms of numerics various approximate models are realized in 3D, leading to fascinating figures of wetting processes in computer animation. However, by incorporating all relevant physics, already in the simplest case of a droplet on a rigid substrate, 3D simulations become rare. Current numerical research is on the development of energy-stable schemes for the phase field equations. Examples for simulations of 3D droplets on rigid substrates within a phase field approach can e.g. be found in [3, 10] for a multi-phase field approach without hydrodynamic coupling and a Navier-Stokes-Cahn-Hilliard model with a generalized Navier boundary condition. In terms of solid state dewetting large scale 3D simulations can be found in [25] and [P4, P1].

1.4 Flexible, adaptive and switchable substrates

There are various new emerging areas resulting from the two-way interaction of the droplet and the (soft) substrate and the ability to control the (de)wetting process. The huge increase in literature on (de)wetting over the last 5 years is mainly due to these phenomena and the resulting applications. Some of them can be found in the recent themed issue on *Wetting and Spreading* [53]. They include the possibility to change the contact angle directly by electric or magnetic fields or to modify the bulk properties. Other examples are responds of the substrate to temperature or humidity. Also wrinkling of a soft substrate has been shown to occur due to capillary forces exerted by droplets [23]. A phenomena which has developed to a valuable tool to measure material properties of the film and/or the droplet (or an adhering cell in a biological context) through the orientation and wavelength of the wrinkles. Vice versa also wrinkling structures have an impact on the droplet and allow another way to control the droplet dynamics [40]. Also in cell biology, where the substrate stiffness is known to influence differentiation of stem cells [16], to determine the direction of cell migration [57] or to modify the cell shape [8] influencing the substrate stiffness opens unpredictable possibilities.

Simulations of these effects are only at the very beginning. However, the phase field approach is well suited to incorporate these additional effects. This can be done on various levels, e.g. by making ψ in the substrate term in eq. (4) time-dependent, by considering electro- or ferrofluidic models in the droplet, or similar viscoelastic or elastomer models for the substrate. These models have not been considered in the context of wetting, but they exist and have been simulated also within a phase field approach, in other contexts.

1.5 Own results obtained in the last years

Within the classical setting of (de)wetting on rigid substrates numerical simulations were used to explore the role of nanotopography for the production of omniphobic surfaces. In [P9,P10] the non-wetting and antiadhesive skin surface of springtails (*Collembola*) was analysed and the computationally found optimal topography used in a tunable polymer replication process which enables the production of omniphobic surfaces from intrinsically hydrophilic polymer materials. The simulations in Figure 4 are done in 2D and consider the Cahn-Hilliard-Navier-Stokes equation mentioned above.

Various model extensions for two-phase flow problems in this phase field setting have been considered. They include the interaction with a substrate and dynamics of contact angles. Fig. 5 shows an example for a droplet sliding down on an implicitly described substrate. Other extensions are soluble and insoluble surfactants [59], essential e.g. for Marangoni transport, further extensions consider the incorporation of bending properties [P8], non-Newtonian fluids [31] and surface viscosities [P5], which are relevant in various biological applications related to cells. Figure 6 shows the resulting flow field within a droplet/vesicle on a rigid substrate under shear flow and the influence of surface viscosity. Also particle laden interfaces have been considered [5, 6] to model bijels and Pickering emulsions.

In terms of solid state dewetting large scale computations have been used as a predictive tool to engineer a hybrid top-down/bottom-up self-assembly process of monocrystalline silicon on insulator [P4]. Figure 7 shows the evolution of a square patch with aspect ratio 1:80 for different templates. The model corresponds to the Cahn-Hilliard setting with a degenerate mobility function, described in Section 1.2 and a contact angle of 90° . Modeling and numerical aspects which allow such large scale simulations are discussed in [63] and [P1]. The approach has also been coupled with elasticity in film and substrate and was considered on more complex topographies [P2]. Current research related to solid state dewetting considers templated dewetting of single crystals to assemble on-chip silicon circuits and dewetting by surface attachment limited kinetics, which was proposed in [11] but never observed for solid films before. Only combined experimental and simulation results allowed to identify this mass transport mechanism

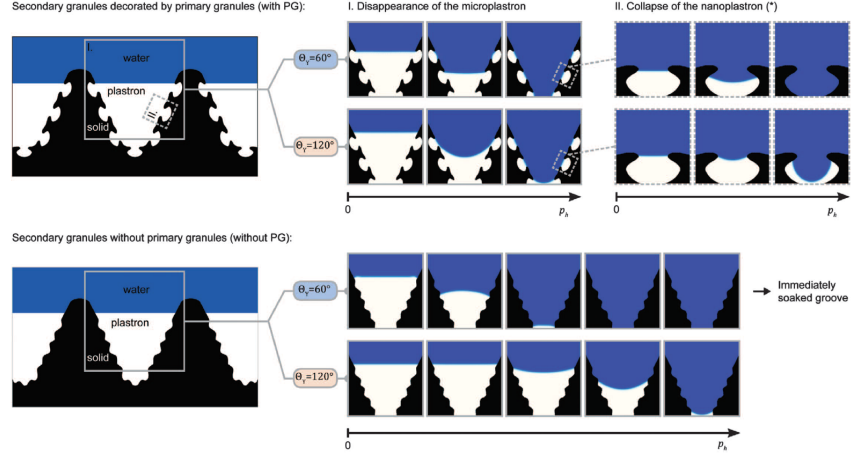


Figure 4: FEM-simulations to explore the dynamics of Cassie-Wenzel transition. On the left hand side, a sectional view through secondary granules that are either decorated by primary granules or not and the initial position of the fluid interface is schematically represented. On the right hand side, numerical results are presented by snap shots from left to right that display the advancing liquid front (blue) displacing the plastron (white) inside certain complex-shaped solid phase fields (black). Both hydrophilic ($\theta = 60^\circ$) and hydrophobic ($\theta = 120^\circ$) surfaces were considered. The hydrostatic pressure difference between the top and bottom boundary was imposed as boundary conditions, which pushes the fluids downwards. From Ref. [P9].

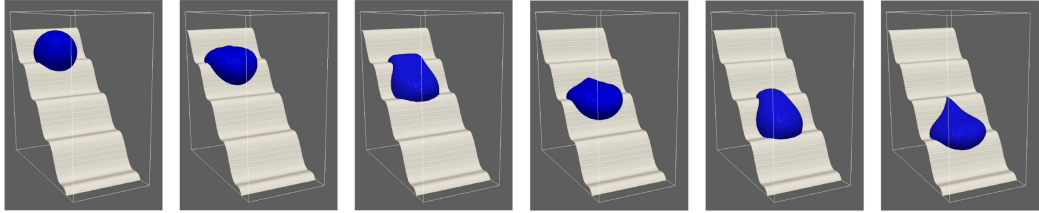


Figure 5: 3D simulation of Navier-Stokes-Cahn-Hilliard model with implicitly defined substrate function ψ and gravitational forces. From Ref. [4].

for silicon films on SiO_2 , see Figure 8. The different mass transport mechanism in liquid and solid thin films will be further explored within the project.

In terms of multi-phase field models we currently consider liquids with large density contrast and volumetric source terms. We thereby compare volume- and mass-averaged velocities and develop energy-stable discretization schemes which scale on high performance computers. Figure 9 shows simple examples of three liquids, establishing Neumann's triangle relation. Within a joint project with the University of Tennessee the simulation code will be installed at the high performance computing facility at Oak Ridge National Laboratory (ORNL). Other activities in terms of computational efficiency are on multi-mesh approaches. Here for each variable an adaptively refined mesh is considered and the interaction between different variables done virtually on a common finest mesh. Especially for multi-phase field formulations, where a high resolution is required only within the diffuse interfaces which differ for different phase field variable, this has been proven to reduced the computational workload drastically [30] and [P6]. Models for viscoelastic materials and phase field realizations of the isotropic interface condition without Marangoni stresses in eq. (8) have been considered in [32], resulting from a Master thesis of D. Mokbel at the Institute of Scientific Computing at TU Dresden. The approach uses adaptive mesh refinement and runs in parallel. All these problems and tools are implemented in the adaptive finite element toolbox AMDiS [62] and [P7], which is available under an open source license and used by various research partners. It will be made available and supported for all projects within SPP2171 for predictions, validations and further development.

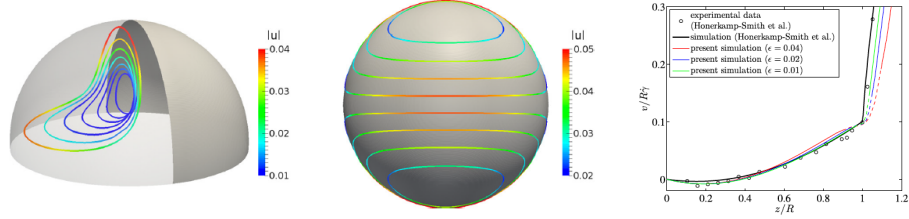


Figure 6: Streamlines of the inner velocity and the surface fluid together with the magnitude of the velocity $|u|$ in a half-spherical drop of radius R subject to shear flow in the outer fluid. The inner velocity profile significantly differs from cases without surface viscosity. Quantitative comparison with experimental/simulation data with v the velocity component parallel to shear flow in the center of the drop and z the height above the substrate. From Ref. [P5].

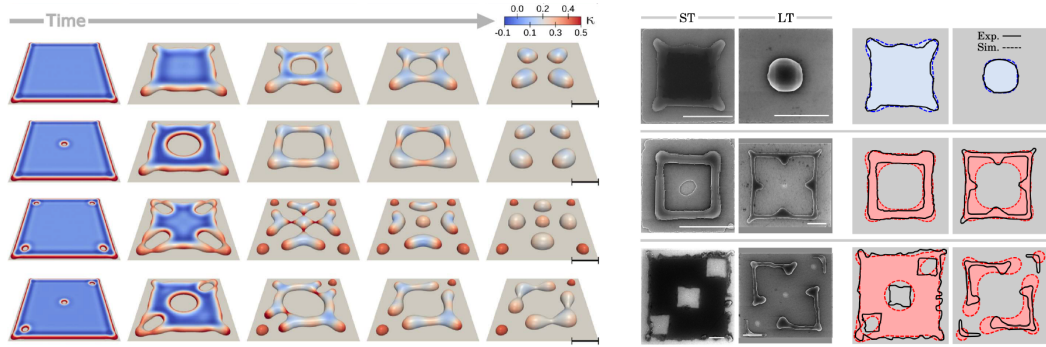


Figure 7: Phase field simulation for solid state dewetting for different templated patches. The color coding corresponds to the curvature. The results are in excellent agreement with the experimental results, showing SEM images for short time (ST) and long time (LT) annealing and comparison with the PF simulations. The colors of the simulated morphologies correspond to different aspect ratios: blue 1:40, red 1:80. From Ref. [P4].

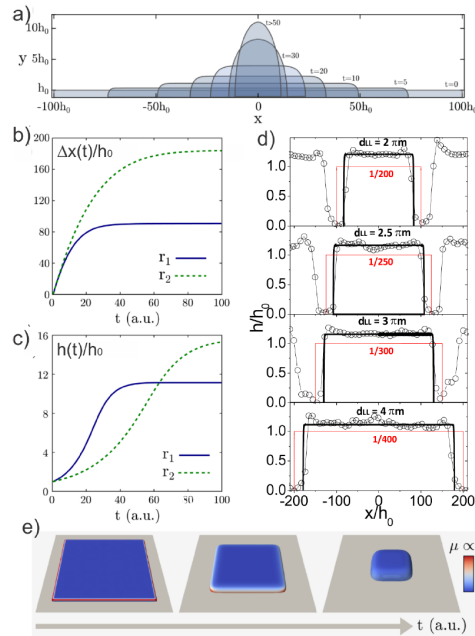


Figure 8: a) Representative stages of evolution of rectangle with aspect ratio 1:200, b) Edge displacement over time for $r_1 = 1 : 200$ and $R_2 = 1 : 400$, c) Increase of thickness over time, d) Comparison between experimental and simulated profiles. The red rectangle is the initial condition, e) phase field simulation for surface attachment limited kinetics with aspect ratio 1:40. Image from M. Naffouti et al. *Shape evolution driven by surface attachment limited kinetics: an unconventional solid-state dewetting scenario*, under review at Phys. Rev. Lett.

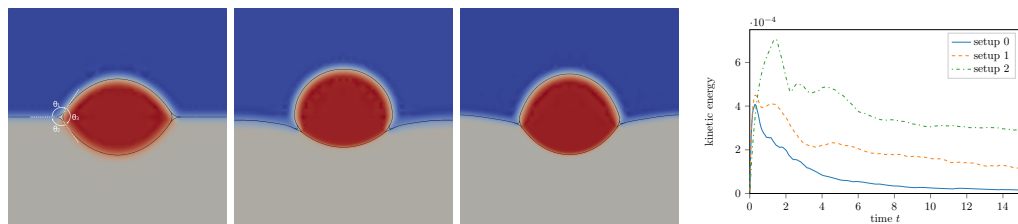


Figure 9: Reached configuration for three liquids, establishing Neumann's triangle relation for (setup 1) density (1:1:1), viscosity (1:1:1) and surface energy (1:1:1) leading to $(121^\circ, 121^\circ, 118^\circ)$. The other cases (setup 2) density (1:1:1), viscosity (1:1:1) and surface energy (10:1:1) leading to $(39^\circ, 165^\circ, 156^\circ)$ and (setup 3) density (1:10:5), viscosity (1:10:100) and surface energy (10:1:1) leading to $(40^\circ, 158^\circ, 162^\circ)$ are not equilibrated as shown in the kinetic energy over time. The angles are extracted from the images using ImageJ and approximate the equilibrium configuration within an error tolerance of 2% which can further be reduced by reducing ϵ .

Other developments consider the derivation of vector- and tensor-valued surface partial differential equations as thin film limits of their 3D counterparts and their numerical solution [34, 36] and [P3]. In [35] a general finite element approach for such problems is derived, which is based on a reformulation in Cartesian coordinates and allows for a componentwise solution using tools for scalar-valued surface partial differential equations such as the surface finite element method [14]. This approach will be essential to solve surface elasticity problems and to determine the strain dependency of the surface stress leading to the Shuttleworth effect [50].

Conference invitations and talks on preliminary results in 2017 and 2018

A. Voigt gave invited talks at the CECAM meeting on "Cell and tissue motility" in Lausanne in 2017, at the Isaac Newton Institute within the program "Growth form and self-organisation" in Cambridge in 2017 and at the MCAIM workshop on "Recent Advances in Applied and Computational Mathematics" in Ann Arbor in 2018. Further talks also by PhD students and PostDocs were given at the DPG spring meeting 2017 in Dresden (A. Voigt, M. Nestler, S. Praetorius) and 2018 in Berlin (A. Voigt, F. Alaimo), the SIAM Conference on Nonlinear Waves and Coherent Structures 2018 in Anaheim (A. Alaimo), the SIAM Conference on Mathematical Aspects in Materials Science 2018 in Portland (A. Voigt, M. Salvalaglio), at WCCM 2018 in New York (A. Voigt), at ICMS in Edinburgh (R. Backofen, M. Salvalaglio), at a GAMM workshop on phase field modeling in Dresden in 2018 (M. Salvalaglio) and at a workshop on "Mathematics of thin film structures" in Dresden in 2018 (M. Nestler) with A. Voigt being one of the organizers. A. Voigt is also invited as plenary speaker of The 4th International Symposium on Phys-Field Modelling in Materials Science (PF19) in Bochum in 2019.

External guests and collaborations

One Humboldt postdoc fellow contributed to the previous work, Dr. Marco Salvalaglio worked on phase field models for solid-state dewetting. Links to experimental colleagues were established with Marco Abbarchi (Marseille), Monica Bollani (Como), Giovanni Capellini (Frankfurt/Oder), Stephan Grill (Dresden), Rene Hensel (Saarbrücken), Moritz Kreysing (Dresden), Christoph Neinhuis (Dresden), Thomas Schröder (Berlin) and Carsten Werner (Dresden). Concerning theoretical aspects close collaborations are established with Andreas Münch (Oxford), Craig Carter (MIT), Harald Garcke (Regensburg), Uwe Thiele (Münster) and Barbara Wagner (Berlin) and links in terms of numerical cooperations exist with Sebastian Aland (Dresden), John Lowengrub (Irvine), Arnold Reusken (Aachen) and Steven Wise (Tennessee).

1.6 Project-related publications

1.6.1 Articles published by outlets with scientific quality assurance

- [P1] R. Backofen, S. M. Wise, M. Salvalaglio, A. Voigt, *Convexity splitting in a phase field model for surface diffusion*, Int. J. Num. Anal. Mod. **16**, 192-209 (2019).
- [P2] M. Salvalaglio, P. Zaumseil, Y. Yamamoto, O. Skibitzki, R. Bergamaschini, T. Schroeder, A. Voigt, G. Capellini, *Morphological evolution of Ge/Si nano-strips driven by Rayleigh-like instability*, Appl. Phys. Lett. **112**, 022101 (2018).
- [P3] I. Nitschke, M. Nestler, S. Praetorius, H. Löwen, A. Voigt, *Nematic liquid crystals on curved surfaces*, Proc. Roy. Soc. London A **474**, 2214 (2018).
- [P4] M. Naffouti, R. Backofen, M. Salvalaglio, T. Bottein, M. Lodari, A. Voigt, T. David, A. Benkoudider, I. Fraj, L. Favre, A. Ronda, I. Berbezier, D. Grosso, M. Abbarchi, M. Bollanii, *Complex dewetting scenarios of ultra-thin silicon films for large-scale nano-architectures*, Science Advances **13**, eaao1472 (2017).
- [P5] S. Reuther, A. Voigt, *Incompressible two-phase flows with an inextensible Newtonian fluid interface*, J. Comput. Phys. **322**, 850-858 (2016).
- [P6] S. Ling, W. Marth, S. Praetorius, A. Voigt, *An adaptive finite element multi-mesh approach for interacting deformable objects in flow*, Comput. Meth. Appl. Math. **16** 475-484 (2016).
- [P7] T. Witkowski, S. Ling, S. Praetorius, A. Voigt, *Software concepts and numerical algorithms for a scalable adaptive parallel finite element method*, Adv. Comput. Math. **41** 1145-1177 (2015).
- [P8] S. Aland, S. Egerer, J. Lowengrub, A. Voigt: *Diffuse interface models of locally inextensible vesicles in a viscous fluid*, J. Comput. Phys. **277** 32-47 (2014).
- [P9] R. Hensel, R. Helbig, S. Aland, A. Voigt, C. Neinhuis, C. Werner, *Tunable nano-replication to explore the omniphobic characteristics of springtail skin*, NPG Asia Mat. **5**, e37 (2013).
- [P10] R. Hensel, R. Helbig, S. Aland, H.-G. Braun, A. Voigt, C. Neinhuis, C. Werner. *Wetting resistance at its topographical limit: The benefit of mushroom and serif T structures*, Langmuir **29**, 1100-1112 (2013).

2 Objectives and work programme

2.1 Anticipated total duration of the project

The anticipated total duration of the project is six years. Support through the DFG will be necessary during the whole period. The present application period is for three years, 1.10.2019 - 30.9.2022.

2.2 Objectives

2.2.1 Modeling

We consider different modeling approaches within a phase field framework, which allow to combine different material properties in the bulk (droplet and substrate) and surface (constant and strain-dependent surface stresses) in a flexible manner.

2.2.1.1 Model extension We extend the phase field approximation of the generalized Oldroyd-B model [32], which models the interface condition eq. (8) in the isotropic setting together with liquid, elastic solid or viscoelastic properties in the bulk phases. It considers

$$\partial_t(\rho_i \mathbf{v}) + \mathbf{v} \cdot \nabla(\rho_i \mathbf{v}) = -\nabla p + \nabla \cdot \boldsymbol{\sigma}_i \quad (10)$$

$$\nabla \cdot \mathbf{v} = 0 \quad (11)$$

in both phases, with phase dependent densities ρ_i and stresses $\boldsymbol{\sigma}_i$ as well as velocity \mathbf{v} and pressure p . The total phase dependent stress is given by an elastic and a viscous part

$$\boldsymbol{\sigma}_i = \mu_i \frac{1}{2}(\mathcal{C} - \mathbf{I}) + \nu_i \frac{1}{2}(\nabla \mathbf{v} + (\nabla \mathbf{v})^T) \quad (12)$$

which models a hyperelastic neo-Hookean material with Green-St-Venant strain tensor $\frac{1}{2}(\mathcal{C} - \mathbf{I})$ and shear modulus μ_i and a Newtonian fluid with deformation tensor $\frac{1}{2}(\nabla \mathbf{v} + (\nabla \mathbf{v})^T)$ and viscosity ν_i . For the Cauchy-Green strain tensor \mathcal{C} it holds in the elastic solid or viscoelastic phase

$$\partial_t \mathcal{C} - (\nabla \mathbf{v})^T \cdot \mathcal{C} - \mathcal{C} \cdot \nabla \mathbf{v} = 0, \quad (13)$$

whereas in the liquid phase $\mathcal{C} = \mathbf{I}$. Within a purely viscous liquid it holds $\mu_i = 0$ and if the elastic solid has no additional viscosity we set $\nu_i = 0$. Within the phase field model the phase field function ϕ interpolates between the different values for ν and μ and considers the equation for the diffuse elastic strain tensor

$$\lambda(\phi)(\partial_t \mathcal{C} - (\nabla \mathbf{v})^T \cdot \mathcal{C} - \mathcal{C} \cdot \nabla \mathbf{v}) + \alpha(\phi)(\mathcal{C} - \mathbf{I}) = 0. \quad (14)$$

For $\alpha = 0$ the equation reduces to the strain evolution for an elastic solid, while for $\lambda = 0$ it reduces to the strain description of a fluid. The case $\alpha = 1$ is known as the Oldroyd-B equation used to model Maxwell-type visco-elasticity with λ being the relaxation time controlling the dissipation of elastic stress. The other equations are of Cahn-Hilliard-Navier-Stokes type, see Section 1.2.

Combining this approach with a substrate energy as in eq. (4) allows to analyze liquid, solid and viscoelastic droplets on rigid substrates. The contact angle in these situations should still fulfill the classical Young's equation.

The second extension considers a multi-phase field approach with three phases to switch between the different phases as in eq. (6) and thus allows to model liquid, solid and viscoelastic droplets on liquid, solid and viscoelastic substrates. The special case of liquid droplets on rigid substrates should lead to the same results as the previous approach and fulfill the classical Young's equation. If soft elastic or viscoelastic properties of the droplet and/or substrate already lead to deviations of the contact angles from Neumann's triangle relation will be analysed.

Both extensions are straight forward and will be done in close cooperation with the project Aland. As the simulation code from [32] is available and realized in AMDIS, this allows already at the beginning of the project to provide a highly flexible computational setting, applicable to various problems considered within SPP2171. However, various effects are still missing and will be the focus of further model extensions.

2.2.1.2 Shuttleworth effect Following [20] the surface of a solid can be modeled as a layer of vanishing thickness adhering to the solid without slipping. The elastic response is governed by

$$-\nabla_\Gamma \cdot \boldsymbol{\Upsilon} = (\boldsymbol{\sigma}_1 - \boldsymbol{\sigma}_2) \cdot \mathbf{n}, \quad \boldsymbol{\mathcal{E}} = \frac{1}{2}(\nabla_\Gamma \mathbf{u} + (\nabla_\Gamma \mathbf{u})^T) \quad (15)$$

with surface strain \mathcal{E} , covariant derivative ∇_Γ and displacement \mathbf{u} . A constitutive law relating surface stress and surface strain reads

$$\mathbf{T} = \gamma \mathbf{I} + 2(\mu_0 - \gamma) \mathcal{E}(\mathbf{u}) + (\lambda_0 + \gamma)(\text{tr}_\Gamma \mathcal{E}(\mathbf{u})) \mathbf{I} + \gamma \nabla_\Gamma \mathbf{u}. \quad (16)$$

It models an elastically isotropic surface with surface Lamé constants λ_0 and μ_0 , surface tension γ and surface identity \mathbf{I} . We propose to solve this problem on general surfaces using the recently developed finite element approach for vector- and tensor-valued surface partial differential equations [35]. In the first step the bulk contribution is thereby given. The numerical approach is based on a Cartesian componentwise description of the covariant derivative of tangential tensor fields, which allows to reformulate the problem in a form suitable to be solved by established tools for scalar-valued surface partial differential equations. The approach has been used for Q -tensors to model surface liquid crystals [P3] and [36] and surface fluids where the constitutive relation between surface stress and surface strain is given by the Boussinesq-Scriven relation [20, 47] $\mathbf{T} = -\pi \mathbf{I} + (\lambda^0 - \nu^0)(\nabla_\Gamma \cdot \mathbf{v}) \mathbf{I} + 2\nu^0 \mathcal{E}(\mathbf{v})$, with surface pressure π (playing the role of γ), interfacial dilatational viscosity λ^0 , interface shear viscosity ν^0 and tangential velocity \mathbf{v} , see [36, 37, 43]. All these realizations consider a surface finite element approach to solve the Cartesian componentwise formulation. This can easily be transformed into a diffuse interface formulation following the general concept proposed in [41] providing a suitable phase-field approach to be coupled with other bulk phenomena and dynamics of the interface. Also extensions to more general elastic surface models are possible within this approach.

2.2.1.3 Elastocapillarity We now extend the phase field approximations derived in Section 2.2.1.1 with the isotropic interface conditions (constant surface stresses) to the general condition in eq. (4). This requires to couple them with the derived phase field model in Section 2.2.1.2. This will allow to model liquid, solid and viscoelastic droplets on liquid, solid and viscoelastic substrates with strain-dependent surface stresses. We will analyze the influence of the Shuttleworth effect for the case of liquid droplets on (soft) elastic substrates, identify parameter regimes where the strain dependency has a strong effect and confirm other theoretical and experimental findings, such as large strains near the contact line [24, 46] or ridge formation [38]. Of interest are also the resulting flow fields in the droplet, which correspond to Marangoni stresses. We plan to compare them and their influence on the contact line, with the corresponding situation of a liquid droplet on a liquid film with surfactants at the film/droplet interface to be considered in the project Hardt/Reusken. A situation which can also be realized within our phase field setting using the extension for soluble and insoluble surfactants in [59].

2.2.1.4 Viscoelastic substrates The considered phase field approach in Section 2.2.1.3 also allows to model viscoelastic Kelvin-Voigt and viscoelastic Maxwell phases. However, a detailed investigation of (viscoelastic) droplets on viscoelastic substrates requires a modification of the elastically isotropic surface. A reasonable modification would be a viscoelastic surface model. The corresponding constitutive law to be used instead of eq. (16) can be derived as a thin film limit from the corresponding bulk model. Similar approaches have been considered for other problems [P3] and [36], a Landau-de Gennes surface model and a surface Navier-Stokes problem, respectively. In terms of elasticity and the derivation of plate and shell models by rigorous analysis we refer to [17, 18]. We will perform this analysis in detail, analyze the effect of the specified boundary conditions at the thin film and the resulting coupling terms with geometric properties and compare the derived model with other phenomenologically proposed approaches by S. Aland.

The coupling with the bulk model follows in the same way as described in Section 2.2.1.3. We will compare the new approach with the (generalized) Shuttleworth effect for viscoelastic substrates with the models in Sections 2.2.1.1 and 2.2.1.3. For liquid droplets on viscoelastic

substrates we are again interested in the developing flow fields in the droplet and their effect on the contact line.

2.2.1.5 Flexible, adaptive and switchable substrates As described in Section 1.4 various possibilities exist to modify properties by external fields. We will only incorporate these effects for specific applications, and otherwise demonstrate the possibilities by effectively varying the surface tension, substrate stiffness or the substrate topography. More detailed investigations in this direction are postponed to the second funding period.

2.2.2 Analysis

Analysis on the derived highly nonlinear partial differential equations will be restricted to matched asymptotics and the derivation of thin-film equations.

2.2.2.1 Matched asymptotics Using formal matched asymptotics we will consider the sharp interface limits as $\epsilon \rightarrow 0$ for the derived phase field models in Section 2.2.1.1, 2.2.1.3 and 2.2.1.4. This extends the analysis in [15] and [P1] to the more general cases taking into account different transport mechanisms, see discussion below eq. (5). The asymptotic analysis will be done in close cooperation with B. Wagner and the resulting models compared with the ones used in the project Seemann/Wagner.

2.2.2.2 Thin film approximation The derived sharp interface models in Section 2.2.2.1 are the basis for a thin film approximation to be considered in the project Seemann/Wagner. However, such approximations are also possible directly for the corresponding phase field models. For simpler situations such approaches have been done in [39], where also a formulation of the disjoining potential was derived. In close cooperation with A. Münch and B. Wagner we will follow this approach and compare the resulting equations with the once derived from the sharp interface models. The similar functional structure of the phase field approach and the thin film model, e.g. in the energy functional, might lead to thin-film models, which are written directly as gradient flows of an underlying energy functional. We will compare the resulting models with the once used in the project Thiele. Following the approach in [39] this might allow to provide effective disjoining potentials for the case of mixtures and surfactants considered in project Thiele.

2.2.3 Numerical approaches

All of the derived phase field models in section 2.2.1 require special care in their numerical treatment. Even if operator splitting approaches and semi-implicit time discretizations typically lead to stable schemes if small time steps are considered, these approaches are far from optimal and not suited for large scale computations. One goal of the project is thus to improve the numerics. All implementations will be done in the parallel adaptive finite element toolbox AMDiS [62] and [P8].

2.2.3.1 Adaptive mesh refinement Due to the different length scales in phase field models, which have to be resolved, adaptive mesh refinement has become a standard tool. This can be done very efficiently due to the a priori knowledge of the refinement region at the diffuse interface. For multi-phase field models this can be combined with a multi-mesh approach, which allows to use differently refined meshes for each phase, see [P7] and [30]. We will use this approach for the three-phase models from Sections 2.2.1, allowing for different refinements of the various interfaces.

The diffuse interface approach for elastically surfaces in Section 2.2.1.2 requires further care. So far we have only experience to solve for surface vector field with such an approach [34]. However, as this approach already contain most of the geometric quantities which need to be computed from the phase field representation, we expect similar behavior also for the surface tensor problem.

To resolve the ridge formation and deviations from Neumann's triangle relation if the Shuttleworth effect (or its generalized version for viscoelastic surfaces) is considered also requires to resolve molecular length scale. The multi-mesh approach will help to keep the resulting computational cost reasonable.

2.2.3.2 Time discretization The best approach to solve the derived phase field models in Section 2.2.1 has to be found out experimentally. We will start from an operator-splitting approach, decoupling the Navier-Stokes-Cahn-Hilliard problem from the Oldroyd-B equation and the surface elasticity problem and consider a semi-implicit time discretization. Improvements can be done using the concepts considered in [P1], an energy-stable convex-splitting approach and higher-order Rosenbrock schemes. In [P1] it is applied together with an appropriate adaptive time-stepping scheme to a Cahn-Hilliard problem with substrate potential to solve large-scale problems in solid state dewetting. The same approach allowed to achieve the agreement with experiments in [P4], see also Figure 7. Such convex-splitting approaches can also be applied to other gradient dynamic problem, as e.g. considered in [60] and will be used for the thin-film models in his project.

2.2.3.3 Preconditioning Various specialized preconditioners have been developed for the Cahn-Hilliard equation and related problems, see [60] for the underlying concept. We plan to adopt this approach to the more general problems and to derived preconditioners for the specific problems derived in Section 2.2.1.

2.2.3.4 Parallelization The simulation code is already parallel, allowing for domain decomposition and parallel solution. All necessary tools are provided in AMDiS, which has demonstrated optimal scaling properties for various phase field models on up to 16.384 cores. In addition to the current installation at the high performance computers in Dresden and Jülich and the available computing hours on these machines, we plan to also use the computing facilities at Oak Ridge National Lab (ORNL), where close collaborations exist with S. Wise.

2.2.3.5 Comparison and benchmark problems Due to the complexity of the problems, lack of analytical solutions and numerical analysis results, a comparison with other simulation approaches is highly desirable. We plan to compare our simulation results with other numerical groups within the SPP2171, especially with the projects Aland, considering an Arbitrary Lagrangian Eulerian (ALE) approach for similar problems, also implemented in AMDiS and the project Hardt/Reusken, using a sharp interface approach within their software package DROPS for liquid droplets. With S. Aland we plan to compare the effect of soft substrates in condensation and dewetting scenarios. With S. Hardt and A. Reusken the effect of insoluble surfactants for liquid droplets on liquid films will be studied using the approach of [59], which has to be adapted to a three-phase field problem.

With all numerical projects within the SPP2171 we plan the definition of suitable benchmark problems. Experience in the setup of benchmark problems for two-phase flow problems exist [7]. Such benchmark problems have also been very successful in the SPP1506, they allow to speedup the development of simulation code, foster an exchange of code between projects in the SPP and have a strong impact for the whole community. With the projects Aland and Hardt/Reusken we plan to define various problems which contain the essential physics, and

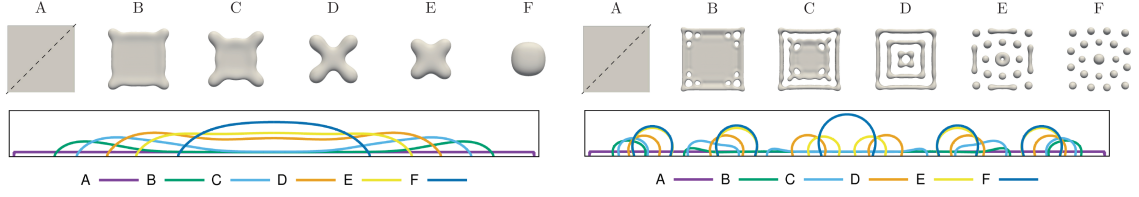


Figure 10: Dewetting of a square island. Change in morphology from left to right and height profile for different stages shown across the diagonal depicted in (A) for eq. (5) with mobility function $M(\phi) = 18\phi^2(1 - \phi)^2$ and contact angle 60° (left) and 120° (right). Image from [P1].

cover the whole spectrum of liquid/viscoelastic/elastic droplets on liquid/viscoelastic/elastic substrates, with and without surfactants and with and without strain-dependent surface stresses. We plan to simulate the relaxation of an initially half-spherical drop on a substrate with three different numerical methods: the ALE method, the ternary phase-field method and a level-set formulation for three viscous phases. The use of realistic physical parameters will ensure that the benchmark is also amenable to experiments, and therefore providing a tool to assess computational modeling errors as well as experimental measurement errors. For dynamic contact angle conditions cooperation is also planned with project Peschka. Within the limit of small contact angles the benchmarks are also suited for the thin film approximations, e.g. considered in projects Seemann/Wagner and Thiele, and can be used for validation.

2.2.4 Simulations

Besides the simulations for single droplets over parameter sets ranging from liquid, viscoelastic and elastic droplets on liquid, viscoelastic and elastic substrates, with constant and strain-dependent surfaces stresses for elastically isotropic or viscoelastic surfaces considered in Section 2.2.1, we will here analyse and compare these effects under different mass transport mechanisms for dewetting scenarios of patches with large aspect ratio, as considered in [P1]. Fig. 10 shows the dewetting of a solid film on a rigid substrate with specified contact angles of 60° and 120° under surfaces diffusion, considering the Cahn-Hilliard type eq. (5) with mobility function $M(\phi) = 18\phi^2(1 - \phi)^2$. The dynamics of these evolutions is rich, including e.g. rupture of the film and merging of droplets, and leads to different morphologies for different contact angles. We plan to classify the resulting morphologies and the dynamics for different settings to answer questions like:

- How does the morphology change with specified contact angle? We systematically vary the contact angle between 60° and 120° .
- What is the influence of the considered mass transport mechanisms? We vary the mobility function, considering $M(\phi) = \epsilon$ for bulk diffusion as in liquids, $M(\phi) = 18\phi^2(1 - \phi)^2$ for surface diffusion as in solids, and various intermediate regimes.
- What is the influence of hydrodynamics within a liquid film? How does the morphology and the dynamics depend on the viscosity ν ? We consider a Cahn-Hilliard-Navier-Stokes equation for the film/vapor system with the substrate interaction and a three-phase field model with a large elastic modulus E in the substrate. Both approaches should lead to the same results.
- How does a liquid film evolve on a liquid substrate? What is the influence of the viscosity ratio? Does a surfactant at the film/substrate interface change the dynamics and the resulting morphology? This investigation will be done in close cooperation with the project Hardt/Reusken.

- What is the influence of elasticity in the substrate? How does the morphology and dynamics depend on the elastic modulus E ? We consider a three-phase field model with one elastic (substrate) and two liquid phases. Especially for soft substrates strong deviations are expected. With increasing softness of the substrate we expect longer relaxation times and probably also prevention of merging [51], which will lead to different morphologies. These aspects will be considered with the project Aland, where similar effects are studied for condensation.
- How does this behavior change if a strain-dependent surface stress is considered. How sensitive is this change with respect to the surface Lamé coefficients μ_0 and λ_0 ?
- What is the effect of a viscoelastic substrate, with and without the (generalized) Shuttleworth effect?
- How does a viscoelastic film evolve on an elastic and viscoelastic substrate?

Answering these questions and validating the results with experimental data, which is planned at least exemplarily with M. Abbarchi for solid thin films and the project Rapp/Helmer for liquid thin films on various substrates, will significantly contribute to a more complete understanding of dewetting for liquid and solid thin films. The formerly distinct research fields will be unified and their similarities and differences explored.

2.3 Work programme incl. proposed research methods

2.3.1 Work programme

In the following we list the steps of investigation that we plan to perform within the first funding period.

W1. Model extension, implementation and simulation for single droplet:

1. Generalized Oldroyd B model with substrate interaction (droplets on rigid substrates), with S. Aland (1 months)
2. Three-phase generalized Oldroyd B model (droplets on soft/viscoelastic/liquid substrates), with S. Aland (2 months)
3. Phase field model for elastically isotropic surface (3 months)
4. Phase field model for elastocapillarity, combining three-phase generalized Oldroyd B model and elastically isotropic surface model (2 months)
5. Extension to include mixtures and surfactants (1 months)
6. Derivation of viscoelastic surface model (3 month)
7. Phase field approximation and coupling with three-phase Oldroyd B model (2 month)

W2. Analytical results for derived phase field model:

1. Sharp interface limit of derived phase field models, with B. Wagner (3 month)
2. Thin film approximation of derived phase field models, with U. Thiele and B. Wagner (3 month)

W3. Numerical improvements to allow for large scale computations:

1. Multimesh concept for three-phase problems (1 months)
2. Energy-stable time discretization for derived phase field models (2 months)

3. Convex splitting scheme for other gradient dynamics approaches, with U. Thiele (2 month)
 4. Development of appropriate problem specific preconditioner (2 month)
 5. Comparison and validation of Marangoni flow induced by Shuttleworth effects and surfactants, with S. Hardt and A. Reusken (2 month)
 6. Comparison between phase field model and ALE discretization, with S. Aland (2 month)
 7. Formulation of benchmark problems, with S. Aland, D. Peschka, A. Reusken, U. Thiele, B. Wagner (3 month)
- W4. Classification of dewetting over whole parameter space:
1. Large scale simulations (9 month)
 2. Experimental validation of dewetting results, with B. Rapp, D. Helmer, R. Seemann (6 months)
- W5. Flexiable, adaptive and switchable substrates:
1. Model adaptation for specific applications to be specified *or*
 2. Demonstration of possibilities by considering time-dependent material properties (4 months)

The intended time line for the project is illustrated in Figure 11.

	2019				2020				2021				2022			
	4	1	2	3	4	1	2	3	4	1	2	3	4	1	2	3
W1.1 - W1.2																
W1.3																
W1.4 - W1.5																
W1.6 - W1.7																
W2.1																
W2.2																
W3.1 - W3.2																
W3.3																
W3.4																
W3.5 - W3.6																
W3.7																
W4.1																
W4.2																
W5																

Figure 11: Time line for the project. The numbers correspond to the items of the work programme as listed above.

2.3.2 Proposed research methods

In all workpackages we consider phase field approximations to model liquid/viscoelastic/elastic droplets on liquid/viscoelastic/elastic substrates. We consider various interface conditions, which range from constant surface energies to isotropic surface elasticity and viscoelastic surfaces. Sharp interface limits and thin film approximations will be derived by formal asymptotic expansions. The phase field models are solved using parallel and adaptive finite element methods together with energy-stable semi-implicit time discretizations, which are implemented in the open-source toolbox AMDiS. All simulations will be performed on high performance computers, at ZIH (Dresden), JSC (Jülich) or ORNL (Tennessee). The models and the simulation results will be validated against known phenomena, other models and numerical approaches, as well as experiments.

2.3.3 Research data and knowledge management

The project will generate resources of high value for the research community. This includes new mathematical models and numerical algorithms. We are fully committed to open access publishing, data and tool sharing policies. This is strongly supported by measures at Technische Universität Dresden (TUD). All challenges to store, process and manage data, are addressed according to the "Guidelines on the Handling of Research Data at TUD". TUD closely cooperates with the Saxon State and University Library (SLUB) and started in 2018 an institutional repository and long-term preservation infrastructure for research data (Project OpARA). This system will be used as the central base for data management for the project. All software tools to be used are open source. For all publications resulting from the project we will follow the DFG guidelines on handling of research data and other typical open data policies of various leading journals and provide access to source code and data to ensure reproducibility of the results.

2.3.4 Synergy with other groups within SPP2171

Synergies are expected from the cooperations which were agreed on during the preparation of the proposal. They include cooperations in model development with **S. Aland**. The phase field approximation of the generalized Oldroyd B model was developed in the Master theses of D. Mokbel at the Institute of Scientific Computing at TU Dresden. D. Mokbel is a research assistant at this institute and is supervised by S. Aland and A. Voigt. Extensions of the model towards substrate interactions and three-phases will be done together. Other modeling aspects consider the sharp interface limit of the derived phase field models. They will be compared with **R. Seemann and B. Wagner**, especially concerning the incorporation of the Shuttleworth effect. With B. Wagner we plan also to work on thin film approximations of the derived phase field models. The resulting models and their structure will be analyzed and compared with other gradient dynamic approaches with **U. Thiele**. Such a derivation might allow to provide effective disjoining potentials for the case of mixtures and surfactants, which will be used by U. Thiele. In terms of numerics various cooperations are planned. They range from comparison of different simulations codes, e.g. an ALE approach (S. Aland) and a sharp interface approach (A. Reusken), to the improvement of discretization schemes for gradient dynamics (U. Thiele), to the definition of benchmark problems, which not only helps the model and algorithms development within the SPP2171, but also will be valuable for the whole community working on simulations of (de)wetting. These benchmarks will be defined together with S. Aland and A. Reusken. Within the limit of small contact angles also groups working on thin film approximations will participate (U. Thiele, B. Wagner). For situations with dynamic contact angle conditions we will in addition work with **D. Peschka**. Concerning experimental validation we cooperate with **S. Hardt and A. Reusken** by considering Marangoni flows and their effect on the contact line, with R. Seemann and B. Wagner by considering the Shuttleworth effect on soft and viscoelastic substrates and **B. Rapp and D. Helmer** to analyse water droplets on various surfaces.

Besides these established cooperations we are open to contribute to other projects where our flexible phase field approach might also be useful. We have considered 4 month in the workprogramme for such additional cooperations.

3 Bibliography

- [1] H. Abels. *Arch. Rat. Mech. Anal.*, 194:463, 2009.
- [2] H. Abels, H. Garcke, and G. Grün. *Math. Mod. Meth. Appl. Sci.*, 22:1150013, 2012.

- [3] S. Aland and F. Chen. *Int. J. Numer. Meth. Fluids*, 91:657, 2016.
- [4] S. Aland, J. Lowengrub, and A. Voigt. *CMES*, 57:77, 2010.
- [5] S. Aland, J. Lowengrub, and A. Voigt. *Phys. Fluids*, 23:062103, 2011.
- [6] S. Aland, J. Lowengrub, and A. Voigt. *Phys. Rev. E*, 86:046321, 2012.
- [7] S. Aland and A. Voigt. *Int. J. Numer. Meth. Fluids*, 69:747, 2012.
- [8] H. E. Balcioglu, H. van Hoorn, D. M. Donato, T. Schmidt, and E. H. J. Danen. *J. Cell Sci.*, 128:1316, 2015.
- [9] J. Becker, G. Grün, R. Seemann, H. Mantz, K. Jacobs, K. Mecke, and R. Blossey. *Nature Materials*, 2:59, 2003.
- [10] M. Ben Said, M. Selzer, B. Nestler, D. Braun, C. Greiner, and H. Garcke. *Langmuir*, 30, 2014.
- [11] W. Carter, A. Roosen, J. Cahn, and J. Taylor. *Acta Metallur.*, 43:4309, 1995.
- [12] S. Dai and Q. Du. *Multisc. Mod. & Sim.*, 12:1870, 2014.
- [13] P.-G. de Gennes, F. Brochard-Wyart, and D. Quere. *Capillarity and wetting phenomena*. Springer, 2004.
- [14] G. Dziuk and C. M. Elliott. *Acta Numerica*, 22:289, 2013.
- [15] M. Dziwnik, A. Münch, and B. Wagner. *Nonlin.*, 30:1465, 2017.
- [16] A. J. Engler, S. Sen, H. L. Sweeney, and D. E. Discher. *Cell*, 126:677, 2006.
- [17] G. Friesecke, R. D. James, M. G. Mora, and S. Müller. *C. R. Acad. Sci. Paris Ser. I*, 336:697, 2003.
- [18] G. Friesecke, R. D. James, and S. Müller. *C. R. Acad. Sci. Paris Ser. I*, 334:173, 2002.
- [19] D. Gentili, G. Foschi, F. Valle, M. Cavallini, and F. Biscarini. *Chem. Soc. Rev.*, 41:4430, 2012.
- [20] M. E. Gurtin and A. I. Murdoch. *Arch. Rat. Mech. Anal.*, 57:291, 1975.
- [21] M. E. Gurtin and A. I. Murdoch. *Int. J. Solids Structures*, 14:431, 1978.
- [22] P. Hansbo and M. Larson. *Comput. Meth. Appl. Mech. Eng.*, 270:1, 2014.
- [23] J. Huang, M. Juszkievicz, W. H. de Jeu, E. Cerda, T. Emrick, N. Menon, and T. P. Russell. *Science*, 317:650, 2007.
- [24] C.-Y. Hui and A. Jagota. *Soft Matter*, 11:8960, 2015.
- [25] W. Jiang, W. Bao, C. V. Thompson, and D. J. Srolovitz. *Acta Mater.*, 60:5578, 2012.
- [26] T. Kajiya, A. Daerr, T. Narita, L. Royon, F. Lequeux, and L. Limat. *Soft Matter*, 9:454, 2013.
- [27] S. Karpitschka, S. Das, M. van Gorcum, H. Perrin, B. Andreotti, and J. H. Snoeijer. *Nature Comm.*, 6, 2015.
- [28] X. Li, J. Lowengrub, A. Rätz, and A. Voigt. *Comm. Math. Sci.*, 7:81, 2009.
- [29] J. Lowengrub and L. Truskinovsky. *Proc. Roy. Soc. A*, 454:2617, 1998.

- [30] W. Marth, S. Aland, and A. Voigt. *J. Fluid Mech.*, 790:389, 2016.
- [31] W. Marth, S. Praetorius, and A. Voigt. *J. Roy. Soc. Interf.*, 12:20150161, 2015.
- [32] D. Mokbel, H. Abels, and S. Aland. *J. Comput. Phys.*, 372:823, 2018.
- [33] P. Muller and A. Saul. *Surf. Sci. Rep.*, 54:157, 2004.
- [34] M. Nestler, I. Nitschke, S. Praetorius, and A. Voigt. *J. Nonl. Sci.*, 28:147, 2018.
- [35] M. Nestler, I. Nitschke, and A. Voigt. *arXiv:1809.00945*.
- [36] I. Nitschke, S. Reuther, and A. Voigt. *arXiv:1809.00457*.
- [37] I. Nitschke, A. Voigt, and J. Wensch. *J. Fluid Mech.*, 708:418, 2012.
- [38] S. Park, B. Wen, J. Lee, J. Lee, J. Kim, and J. Je. *Nature Comm.*, 5:4369, 2014.
- [39] L. Pismen and Y. Pomeau. *Phys. Rev. E*, 62:2480, 2000.
- [40] R. Prathapan, J. D. Berry, A. Fery, G. Garnier, and R. F. Tabor. *ACS Appl. Mater. & Interf.*, 9:15202, 2017.
- [41] A. Rätz and A. Voigt. *Comm. Math. Sci.*, 4:575, 2006.
- [42] S. Reuther and A. Voigt. *Multisc. Mod. Sim.*, 13(2):632, 2015.
- [43] S. Reuther and A. Voigt. *Phys. Fluids*, 30:012107, 2018.
- [44] M. S. Roudbari, G. Simsek, E. H. van Brummelen, and K. G. van der Zee. *Math. Mod. Meth. Appl. Sci.*, 28:733, 2018.
- [45] D. Schöllhammer and T.-P. Fries. *arXiv:1805.11978*.
- [46] R. D. Schulman and K. Dalnoki-Veress. *Phys. Rev. Lett.*, 115, 2015.
- [47] L. Scriven. *Chem. Eng. Sci.*, 12:98, 1960.
- [48] M. Shanahan and A. Carre. *Langmuir*, 11:1396, 1995.
- [49] Y. Shikhmurzaev. *Capillary flows with forming interfaces*. Chapman & Hall, 2007.
- [50] R. Shuttleworth. *Proc. Phys. Soc. London A*, 63:444, 1950.
- [51] M. Sokuler, G. K. Auernhammer, M. Roth, C. Liu, E. Bonaccorso, and H.-J. Butt. *Langmuir*, 26:1544, 2010.
- [52] J. E. Sprittles and Y. D. Shikhmurzaev. *J. Comput. Phys.*, 233:34, 2013.
- [53] V. Starov and H.-J. Butt. *Curr. Opt. Colloid Surf. Sci.*, 36:A1, 2018.
- [54] I. Steinbach. *Ann. Rev. Mat. Res.*, 43:89–107, 2013.
- [55] R. Style, A. Jagota, C.-Y. Hui, and E. Dufresne. *Ann. Rev. Cond. Matt. Phys.*, 8:99, 2017.
- [56] R. W. Style, Y. Che, S. J. Park, B. M. Weon, J. H. Je, C. Hyland, G. K. German, M. P. Power, L. A. Wilen, J. S. Wettlaufer, and E. R. Dufresne. *Proc. Nat. Acad. Sci. USA*, 110:12541, 2013.
- [57] R. Sunyer, V. Conte, J. Escribano, A. Elosegui-Artola, A. Labernadie, L. Valon, D. Navajas, J. Manuel Garcia-Aznar, J. J. Munoz, P. Roca-Cusachs, and X. Trepate. *Science*, 353:1157, 2016.

- [58] K. E. Teigen, X. Li, J. Lowengrub, F. Wang, and A. Voigt. *Comm. Math. Sci.*, 7:1009, 2009.
- [59] K. E. Teigen, P. Song, J. Lowengrub, and A. Voigt. *J. Comput. Phys.*, 230:375, 2011.
- [60] U. Thiele. *Colloids Surf. A*, 553:487, 2018.
- [61] C. Thompson. *Ann. Rev. Mater. Res.*, 42:399, 2012.
- [62] S. Vey and A. Voigt. *Comput. Vis. Sci.*, 10:57, 2007.
- [63] A. Voigt. *Appl. Phys. Lett.*, 108:036101, 2016.
- [64] A. Yavari, A. Ozakin, and S. Sadik. *J. Nonlin. Sci.*, 26:1651, 2016.

4 Requested modules/funds

4.1 Basic Module

4.1.1 Funding for Staff

One PostDoc on a **1.0 TVL-13 position** is needed to perform the research project in its full breadth including the theoretical development, the numerical implementation, large scale simulations, data handling and the interaction with the experimental groups with the SPP. Dr. Marco Salvalaglio, currently Humboldt fellow at the Institute of Scientific Computing, is intended to fill this position. He was e.g. involved in [P1,P2,P4], see also attached CV.

4.1.2 Direct Project Costs

4.1.2.1 Travel Expenses

Euro 3400 per year is necessary for

- a) two short exchange visits with other groups in the SPP per year for the principle investigator and the PostDoc (400 Euro per trip) which sums up to Euro 800 per year.
- b) specific exchange visits e.g. to the scientists mentioned below: about one short contact visit per year à Euro 500 for the principal investigator and the PostDoc, which sums up to Euro 1000 per year.
- c) the attendance of one international conference per year (SIAM meetings, MRS meetings, CECAM workshops, Gordon conferences) for the principal investigator and the PostDoc. Each conference costs about Euro 800. This sums up to about Euro 1600 per year.

4.1.2.2 Visiting Researchers

Euro 1000 per year for invitations of external guest scientists for short-term visits. We intend to invite scientists with whom we collaborate within the proposal. Among those are Marco Abbarchi (Marseille), Ken Elder (Oakland) and Steven Wise (Tennessee). The costs will cover travel and local accommodation.

4.1.2.6 Project-related publication expenses

Euro 750 per year for publication charges for papers which result from the research within the current project.

5 Project requirements

5.1 Employment status information

Voigt, Axel, Professor Dr., Professor W3.

5.2 Composition of the project group

In addition to the project leader, Dr. Simon Praetorius and the PhD student Ingo Nitschke funded from TU Dresden will participate in the project. In particular they will further develop the finite element software AMDiS to allow for efficient simulations of the PF models. Computer administration will be assisted by ZIH and secretary support will be provided by Mrs. Cindy Röhling (0.5 TVL E7). Additional Master and Bachelor students will further participate in the project with appropriate research subprojects.

5.3 Cooperation with other researchers

5.3.1 Researchers with whom you have agreed to cooperate on this project

- a) Existing collaborations all proven by recent joint publications which are essential also for the project are with Ken Elder (Oakland), Sebastian Aland (Dresden), Stephan Grill (Dresden), Steven Wise (Tennessee). We have also agreed to collaborate with Thomas-Peter Fries (Graz), Dirk Peschka (Berlin), Arnold Reusken (Aachen) and Uwe Thiele (Münster) on numerical aspects of the derived equations.
- b) We shall keep a close contact to experimentalists. We have discussed our results in the past and are in contact with the following experimental scientists: Marco Abbarchi (Marseille), Jochen Guck (Dresden), Stephan Grill (Dresden), Moritz Kreysing (Dresden), Christoph Neinhuis (Dresden), Carsten Werner (Dresden). We have also agreed to collaborate with Ralf Seemann (Saarbrücken).
- c) Discussions and collaborations regarding the modelling aspects were done in the past with Ken Elder (Oakland), Andreas Münch (Oxford), Len Pismen (Haifa), Uwe Thiele (Münster) and Barbara Wagner (Berlin). These are planned to be extended throughout the project.

5.3.2 Researchers with whom you have collaborated scientifically within the past three years

M. Abbarchi, S. Aland, T. Ala-Nissila, S. Alberti, V. Alt, M. Bollani, K. Barmak, C. Carter, G. Capellini, K. Eckert, K. Elder, S. Franz, D. Grosso, M. Gude, J. Fröhlich, S. Grill, J. Guck, H. Hatzikirou, C. Heiss, J. Howard, G. Isella, M. Kreysing, J. Lowengrub, L. Miglio, F. Montalenti, G. Napoli, C. Nienhuis, K. Padberg-Gehle, A. Rätz, A. Reusken, M. Rohnke, S. Sadik, T. Sakayo, T. Schröder, J. Wensch, C. Werner, S. Wise, R. Wittkowski.

5.4 Scientific equipment

Access to high performance clusters at ZIH and Jülich is available and will be provided to perform the PF simulations. Further resources for large scale computations will be available at ORNL.

6 Additional information

A request for funding of this proposal has not been submitted to any other addressee. In the event that I submit such a request, I will inform the Deutsche Forschungsgemeinschaft immediately. In submitting a proposal for a research grant to the DFG, I agree to adhere to the DFG's rules of good scientific practice. In preparing our proposal, I have adhered to the guidelines for publication lists and bibliographies. The DFG liaison officers of the TU Dresden was informed about this application.